PHYSICAL REVIEW C **79**, 041301(R) (2009)

Quenching of Gamow-Teller strength due to tensor correlations in ^{90}Zr and ^{208}Pb

C. L. Bai,[1,2] H. Q. Zhang,[1,2] X. Z. Zhang,[2] F. R. Xu,[1] H. Sagawa,[3] and G. Colò[4]

[1]*School of Physics and State Key Laboratory of Nuclear Physics and Technology, Peking University, People's Republic of China*

[2]*China Institute of Atomic Energy, People's Republic of China*

[3]*Center for Mathematical Sciences, University of Aizu, Aizu-Wakamatsu, Fukushima 965-8560, Japan*

[4]*Dipartimento di Fisica, Università degli Studi and INFN, Sezione di Milano, IT-20133 Milano, Italy*

(Received 19 March 2009; published 24 April 2009)

We performed self-consistent Hartree-Fock plus random-phase approximation (HF+RPA) calculations for charge-exchange 1^+ states in ^{90}Zr and ^{208}Pb by using Skyrme interactions with tensor terms. We employed a parameter set in which the tensor terms are added to the SGII interaction. It is pointed out that Gamow-Teller (GT) states can couple strongly with the spin-quadrupole (SQ) 1^+ states in the high-energy region above $E_x = 30$ MeV due to the tensor interactions. As a result of this coupling, more than 10% of the GT strength is shifted to the energy region above 30 MeV, and the main GT peak is moved 2 MeV downward. At the same time, the main SQ 1^+ peak is moved upward by more than 10 MeV due to the tensor correlations. Schematic separable interactions are proposed to elucidate the quenching mechanism induced by the tensor interaction on the GT state.

DOI: 10.1103/PhysRevC.79.041301 PACS number(s): 21.10.Ky, 21.30.Fe, 21.60.Jz, 24.30.Gd

Spin and spin-isospin excitation modes give a unique opportunity to study the spin correlations in nuclei [1–3]. A systematic study of the energy and the collectivity of these modes gives not only direct information on the spin and isospin properties of the nuclear interaction, but also on the equation of state of asymmetric nuclear matter. It is claimed that the neutron skin thickness is determined indirectly by the excitation energy spacing between the isobaric analog state and Gamow-Teller (GT) resonances [4]. More generally, spin collective resonances are deeply related to several fundamental problems of interdisciplinary fields, such as the description of neutron stars and supernova explosions, the β decay of nuclei along the r-process path of stellar nucleosynthesis, and the efficiency of solar neutrino detectors.

It has been known that the random-phase approximation (RPA) is an appropriate microscopic model for charge-exchange giant resonances [5]. The self-consistency is an extremely important requirement for the analysis of long isotopic chains toward the drip line and the predictions of new collective modes in unstable nuclei without introducing any adjustable parameter. So far, Skyrme-RPA calculations without the tensor interactions have been carried out for the charge-exchange excitations [6,7]. Recently, the importance of the tensor terms in Skyrme interactions has been recognized in the study of the shell evolution of single-particle states along isotopic or isotonic chains [8–10]. In the self-consistent Hartree-Fock plus random-phase approximation (HF+RPA) model, zero-range tensor terms were introduced to study the effects of tensor forces on the GT transitions [11]. The important findings are that about 10% of the GT strength is shifted to the excitation energy region above 30 MeV (with respect to the ground state of the target nucleus) already at the 1p-1h level, and the main GT peak is moved downward by about 2 MeV by RPA tensor correlations. The present work is devoted to finding out the mechanism underlying this redistribution of multipole strength, as well as to studying the spin-quadrupole excitations. We employ here the same zero-range tensor interaction as that in our previous work [11], namely,

$$V^T = \frac{T}{2}\left\{\left[(\sigma_1\cdot\mathbf{k}')(\sigma_2\cdot\mathbf{k}') - \frac{1}{3}(\sigma_1\cdot\sigma_2)\,\mathbf{k}'^2\right]\delta(\mathbf{r}) + \delta(\mathbf{r})\left[(\sigma_1\cdot\mathbf{k})(\sigma_2\cdot\mathbf{k}) - \frac{1}{3}(\sigma_1\cdot\sigma_2)\,\mathbf{k}^2\right]\right\} + \frac{U}{2}\{(\sigma_1\cdot\mathbf{k}')\delta(\mathbf{r})(\sigma_2\cdot\mathbf{k}) + (\sigma_2\cdot\mathbf{k}')\delta(\mathbf{r})(\sigma_1\cdot\mathbf{k}) - \frac{2}{3}[(\sigma_1\cdot\sigma_2)\mathbf{k}'\cdot\delta(\mathbf{r})\mathbf{k}]\}. \quad (1)$$

In this expression, the coupling constants T and U denote the triplet-even and triplet-odd tensor interactions, respectively. The tensor terms lead to a modification to the spin-orbit potential

$$U^{(q)}_{\text{S.O.}} = \frac{W_0}{2r}\left(2\frac{d\rho_q}{dr} + \frac{d\rho_{q'}}{dr}\right) + \left(\alpha\frac{J_q}{r} + \beta\frac{J_{q'}}{r}\right), \quad (2)$$

where the $J_q(\mathbf{r})(q = p, n)$ are spin-orbit densities, whereas α and β are composed of the central-exchange and tensor contributions, that is, $\alpha = \alpha_C + \alpha_T$ and $\beta = \beta_C + \beta_T$ with

$$\alpha_C = \frac{1}{8}(t_1 - t_2) - \frac{1}{8}(t_1x_1 + t_2x_2), \quad (3)$$

$$\beta_C = -\frac{1}{8}(t_1x_1 + t_2x_2), \quad (4)$$

$$\alpha_T = \frac{5}{12}U, \quad (5)$$

$$\beta_T = \frac{5}{24}(T + U). \quad (6)$$

As the parameter set, we use the Skyrme force SGII, which is among those appropriate for the description of spin-dependent properties of nuclei. For the force SGII, $\alpha_c = 57.7$ MeV fm^5 and $\beta_c = 10.0$ MeV fm^5. Taking into account the contributions α_c and β_c, we have chosen for the tensor terms the values $\alpha_T = -180$ MeV fm^5 and $\beta_T = 120$ MeV fm^5, which are practically the same as those of the previous publications [8,10,11]. It should be noted that J_q gives essentially no contribution in the spin-saturated cases. As in Ref. [11], we choose ^{90}Zr and ^{208}Pb as examples to be calculated, because ^{90}Zr is a proton spin-saturated nucleus with a spin-unsaturated neutron $1g$ orbit and ^{208}Pb is a spin-unsaturated nucleus both for protons or neutrons.

For spin-dependent excitations with a given angular momentum λ and parity $(-)^{\lambda+1}$, there are always two excitation modes specified by the orbital angular momentum $l = \lambda \pm 1$: one is associated with the operator $[r^{\lambda-1}Y_{\lambda-1}\sigma_1]_\lambda$ and has a lower average excitation energy, while the other one is associated with the operator $[r^{\lambda+1}Y_{\lambda+1}\sigma_1]_\lambda$ and is characterized by higher average excitation energy than the former one by about $2\hbar\omega$. It was suggested [13] that the interaction term $[(Y_0(1)\sigma_1(1))_1(r^2Y_2(2)\sigma_1(2))_1]_0$, which is associated with the tensor force, produces a coupling between the lower and the higher magnetic λ-pole excitation mode, as in the well-known case of the deuteron ground state [12].

For the spin-dependent charge-exchange 1^+ modes, we consider two kinds of excitations:

$$\hat{O}_{\mathrm{GT}\pm} = \sum_i t^i_\pm \sigma^i_1 = \sqrt{4\pi}\sum_i t^i_\pm \left(Y_0\sigma^i_1\right)^1, \qquad (7)$$

$$\hat{O}_{\mathrm{SQ}\pm} = \sum_i t^i_\pm \left(r_i^2 Y_2^i \sigma^i_1\right)^1, \qquad (8)$$

where the first one produces the GT excitation and the second one produces the spin-quadrupole (SQ) excitation.

The calculated unperturbed GT_- and SQ_- strength distributions in ^{90}Zr and ^{208}Pb are displayed in Fig. 1. Results labeled as '00' or '11' correspond to the ones without or with the tensor term [Eq. (1)] in the HF calculations. As shown in the figure, the unperturbed GT strength is distributed in the energy region below 20 MeV (low frequency) for both nuclei ^{90}Zr and ^{208}Pb. On the other hand, the strengths of SQ_- are distributed in two regions: one with a small portion of SQ_- strength is located in the same region as that of GT_-, while the main 1^+ SQ_- strength is distributed in the region above 30 MeV.

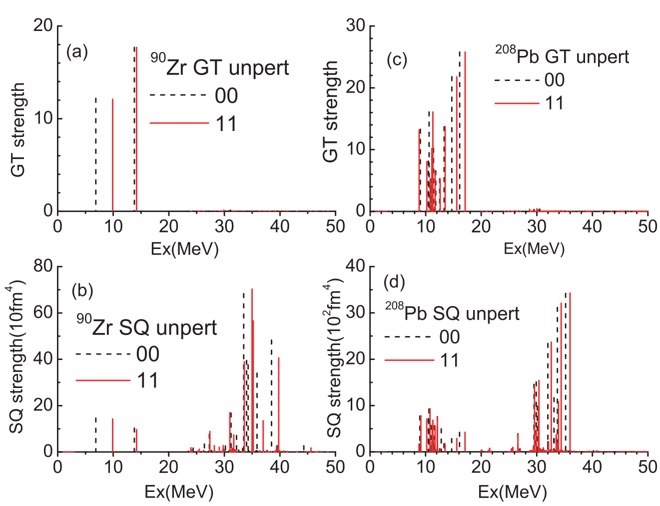

FIG. 1. (Color online) Unperturbed charge-exchange GT_- and 1^+ SQ_- strengths in ^{90}Zr and ^{208}Pb. In panels (a) and (c), the results of GT_- transitions in ^{90}Zr and ^{208}Pb are displayed, respectively. In panels (b) and (d), the results of charge-exchange SQ_- transitions in ^{90}Zr and ^{208}Pb are displayed, respectively. The results without and with tensor terms are labeled as '00' and '11,' respectively.

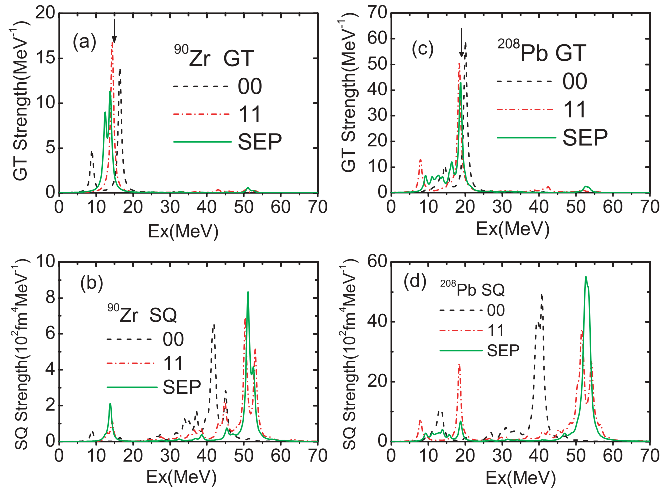

FIG. 2. (Color online) Charge-exchange GT_- and 1^+ SQ_- strength distributions in ^{90}Zr and ^{208}Pb. In panels (a) and (c), the RPA results of GT transitions in ^{90}Zr and ^{208}Pb are displayed, respectively. In panels (b) and (d), the RPA results of charge-exchange SQ transitions in ^{90}Zr and ^{208}Pb are displayed, respectively. The curves corresponding to the results with and without the tensor terms in both HF and RPA are labeled as '11' and '00,' respectively. Those calculated with the separable interaction [Eq. (9)] for RPA are labeled SEP. The discrete RPA peaks have been smoothed by using a Lorentzian averaging with width 1 MeV. The arrow corresponds to the experimental energy [14]. See the text for details.

In the present work, HF and RPA calculations have been performed for the charge-exchange 1^+ states in ^{90}Zr and ^{208}Pb with and without the tensor interactions. The results for the GT_- and 1^+ SQ_- strength distributions are shown in Fig. 2. The results without tensor terms are labeled by '00', while those with tensor terms in both HF and RPA calculations are labeled by '11'. In the RPA calculations, the two-body spin-orbit interaction is not included, but its effect on the final result was shown to be negligible for the GT excitations [7]. The energy shift caused by the tensor force in the two nuclei are calculated by using the RPA calculations and the analytic formula in Ref. [11]. The results are displayed in Table I. Good agreement in the energy shift calculated by the two methods

TABLE I. Energy weighted sum rule (EWSR) $m_- + m_+(1)$ obtained by the self-consistent HF+RPA calculations with and without the tensor terms. δE_{RPA} and δE_{DC} are the contributions of the tensor terms to the calculated GT centroid energy, respectively, by using RPA and the analytical formula in Ref. [11]. All values are in MeV.

	$m_- + m_+(1)$ no tensor	$m_- + m_+(1)$ with tensor	δE_{RPA}	δE_{DC}
^{90}Zr	469	547	2.6	2.66
^{208}Pb	2524	2690	1.26	1.3

indicates that the self-consistency is quite well preserved in the numerical calculations.

From Fig. 2, three points should be noticed. First, more than 10% of the GT_- strength has been shifted from the low-energy region to the energy region above 30 MeV by the tensor correlations. Second, the high frequency 1^+ SQ strengths are moved upward more than 10 MeV for both ^{90}Zr and ^{208}Pb by the tensor correlations. Adding tensor terms to the SGII force, the peak of the calculated excitation strength of the GT transition becomes quite close to the experimental results obtained by $^{90}\mathrm{Zr}(p,n)^{90}\mathrm{Nb}$ reactions. Third, most of the GT_- strengths appearing in the energy region above 30 MeV coincide with the peaks of the 1^+ SQ_- strengths. This coincidence indicates possible strong coupling between the low-frequency GT_- excitations and the high-frequency 1^+ SQ_- excitations by the tensor interactions.

To understand the effect of tensor forces on GT_- and 1^+ SQ_- excitations in a more transparent way, we simulate the main effects of tensor correlations by a separable interaction

$$V_{\mathrm{SEP}} = \lambda_1 \sum_{\mu} \big[(Y_0(1)\sigma_1(1))_{1\mu} \left(r_2^2 Y_2(2)\sigma_1(2)\right)^+_{1\mu} + \left(r_1^2 Y_2(1)\sigma_1(1)\right)_{1\mu} (Y_0(2)\sigma_1(2))^+_{1\mu} \big] \tau_1 \cdot \tau_2 + \lambda_2 \sum_{\mu} \left(r_1^2 Y_2(1)\sigma_1(1)\right)_{1\mu} \left(r_2^2 Y_2(2)\sigma_1(2)\right)^+_{1\mu} \tau_1 \cdot \tau_2 \qquad (9)$$

in the RPA calculations. Taking the coupling constants λ_1 and λ_2 as adjustable parameters, we performed RPA calculations for ^{90}Zr and ^{208}Pb by replacing the Skyrme tensor terms by this two-term separable interaction. The calculated results are displayed in Fig. 2 with the label SEP. We can see in this figure that the global features of tensor effects on both GT_- and 1^+ SQ_- strength distributions can be well accounted for by using the two-term separable interaction. For ^{90}Zr, the coupling constants $\lambda_1 = 0.16$ MeV fm^{-2} and $\lambda_2 = 0.0043$ MeV fm^{-4} are chosen for the RPA calculations. The results with the separable forces mimics well those of Skyrme tensor terms labeled as '11' in Fig. 2; i.e., the main peak of 1^+ SQ_- strength appears at $E_x \sim 51$ MeV, and more than 7% of the GT_- strength is shifted to this energy region by the RPA correlations induced by the separable interaction. For the nucleus ^{208}Pb, we choose the coupling constants $\lambda_1 = 0.029$ MeV fm^{-2} and $\lambda_2 = 0.00087$ MeV fm^{-4}. In this case also, the SEP results are similar to those of Skyrme plus tensor labeled as '11'; namely, the main 1^+ SQ peak appears at $E_x \sim 52.6$ MeV, and about 8% of the GT strength is shifted to this energy region by the RPA correlations coming from the separable interactions.

To study more specifically the effects of the separable interactions, RPA calculations were done by using λ_1 and λ_2 terms, separately. In Fig. 3, the GT_- and charge-exchange 1^+ SQ_- strength distributions in ^{90}Zr and ^{208}Pb are displayed. Results labeled as $\lambda_1(\lambda_2)$ correspond to those using only the term $\lambda_1(\lambda_2)$. The SEP results are the same as shown in Fig. 2. It is clearly seen that the λ_1 term couples GT with 1^+ SQ excitations so that 7% or 8% of the total GT strength is shifted to the region around the high-energy peak of 1^+ SQ excitations in ^{90}Zr and ^{208}Pb, respectively. While the coupling term λ_1 has only a minor effect on the 1^+ SQ excitations, the GT strength distribution is moved downward by the coupling to the 1^+ SQ excitations. While the λ_2 term does not make any appreciable coupling between GT and SQ modes, the dominant peaks of SQ excitations are shifted to substantially higher energy, close to the SEP results, and take part of the low-energy 1^+ SQ strengths to the high-energy region.

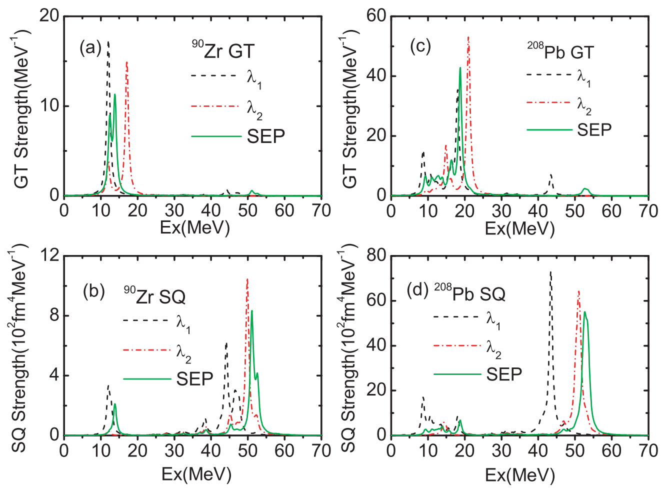

FIG. 3. (Color online) Charge-exchange GT_- and 1^+ SQ_- strengths in ^{90}Zr and ^{208}Pb. In panels (a) and (c), the RPA results of GT transitions in ^{90}Zr and ^{208}Pb are displayed, respectively. In panels (b) and (d), the RPA results of charge-exchange SQ transitions in ^{90}Zr and ^{208}Pb are displayed, respectively. The separable interaction [Eq. (9)] is adopted in the RPA calculations, while HF calculations are performed by using the Skyrme tensor terms [Eq. (1)]. The RPA calculations are performed in three different ways: only the λ_1 term (labeled λ_1); only the λ_2 term (labeled λ_2); both λ_1 and λ_2 terms (labeled SEP). The discrete RPA peaks have been smoothed by using a Lorentzian averaging with width 1 MeV. See the text for details.

In summary, we studied the effects of the tensor interactions on the GT_- and charge-exchange 1^+ SQ_- excitations in the self-consistent HF+RPA calculations. The tensor interactions are taken into account on top of the Skyrme parameter set SGII. Without the tensor forces, all the GT strength is distributed in the energy region below 30 MeV, while the strength of 1^+ SQ_- excitations are distributed in two energy regions: a small portion is in the same energy region as the GT strength, whereas the main portion of the strength appears above 40 MeV. When the tensor force is included, more than 10% of the GT strength is shifted from the low-energy region to the energy region above 30 MeV, and the main peak of GT strength is moved downward by about 2 MeV. Concerning the 1^+ SQ excitations, the tensor force moves most of their strength in the high-energy region. It is pointed out that the GT peaks in the energy region above 30 MeV in most cases correspond to the peaks of the 1^+ SQ strength, indicating the strong coupling between these two excitation modes that is produced by the tensor forces. We introduced a simple separable interaction with two terms λ_1 and λ_2 in the RPA calculation to elucidate the role of the tensor correlations on the spin-dependent excitations. The main results obtained with the Skyrme set plus the tensor force are reproduced pretty well. The λ_1 term couples the low-frequency GT mode and the high-frequency 1^+ SQ mode, shifting 7% or 8% of the total GT strength to the high-energy region of the 1^+ SQ excitations, and the λ_2 term pushes the 1^+ SQ excitations to even higher energy. The main peak of GT strength moves downward by about 2 MeV due to the net effect of the λ_1 and λ_2 terms.

This work is supported by the National Natural Science Foundation of China under Grant Nos. 10875172, 10275092, and 10675169 and the National Key Basic Research Program of China under Grant No. 2007CB815000.

[1] M. N. Harakeh and A. M. van der Woude, *Giant Resonances: Fundamental High-Frequency Modes of Nuclear Excitation* (Oxford University Press, Oxford, 2001).
[2] F. Osterfeld, Rev. Mod. Phys. **64**, 491 (1992).
[3] M. Ichimura, H. Sakai, and T. Wakasa, Prog. Part. Nucl. Phys. **56**, 446 (2006).
[4] D. Vretenar, N. Paar, T. Nikšić, and P. Ring, Phys. Rev. Lett. **91**, 262502 (2003).
[5] N. Auerbach, A. Klein, and N. Van Giai, Phys. Lett. **B106**, 347 (1981).
[6] I. Hamamoto and H. Sagawa, Phys. Rev. C **62**, 024319 (2000); H. Sagawa, Satoshi Yoshida, Xian-Rong Zhou, K. Yako, and H. Sakai, *ibid*. **76**, 024301 (2007).
[7] S. Fracasso and G. Colò, Phys. Rev. C **76**, 044307 (2007).
[8] B. A. Brown, T. Duguet, T. Otsuka, D. Abe, and T. Suzuki, Phys. Rev. C **74**, 061303(R) (2006).
[9] D. M. Brink and Fl. Stancu, Phys. Rev. C **75**, 064311 (2007).
[10] G. Colò, H. Sagawa, S. Fracasso, and P. F. Bortignon, Phys. Lett. **B646**, 227 (2007).
[11] C. L. Bai, H. Sagawa, H. Q. Zhang, X. Z. Zhang, G. Colò, and F. R. Xu, Phys. Lett. **B675**, 28 (2009).
[12] J. M. Blatt and V. F. Weisskopf, *Theoretical Nuclear Physics* (John Wiley & Sons, Inc., New York, 1952), p. 97.
[13] H. C. Chang, Phys. Lett. **B69**, 272 (1977).
[14] T. Wakasa *et al.*, Phys. Rev. C **55**, 2909 (1997); C. Gaarde, J. S. Larsen, A. G. Drentje, M. N. Harakeh, and S. Y. van der Werf, Phys. Rev. Lett. **46**, 902 (1981).